International Journal of Nanomedicine

Dovepress
open access to scientific and medical research

Open Access Full Text Article

ORIGINAL RESEARCH

A chemoenzymatically synthesized cholesterol-g-poly(amine-co-ester)-mediated *p53* gene delivery for achieving antitumor efficacy in prostate cancer

This article was published in the following Dove Medical Press journal:
International Journal of Nanomedicine

Mengmeng Dong[1,2,*]
Jiawen Chen[2,*]
Jiayuan Zhang[2]
Xiao Liang[2]
Jiebing Yang[2]
Dan Li[1]
Quanshun Li[2]

[1]Department of Cancer Center, The First Hospital of Jilin University, Changchun 130021, People's Republic of China; [2]Key Laboratory for Molecular Enzymology and Engineering of Ministry of Education, School of Life Sciences, Jilin University, Changchun 130012, People's Republic of China

*These authors contributed equally to this work

Background: An amphiphilic cationic copolymer cholesterol-g-poly(amine-co-ester), namely Chol-g-PMSC-PPDL synthesized in a chemoenzymatic route has been utilized as a carrier for *p53* gene delivery to check its antitumor efficacy, using human prostate cancer cell line PC-3 (p53 null) as a model.

Materials and methods: The transfection efficiency was measured by quantitative PCR and Western blotting assay. The anti-proliferative effect was detected using MTT method, colony formation assay and Live/Dead staining. The anti-migration effect was evaluated through wound healing and Transwell migration assays.

Results: The transfection efficiency assay indicated that the carrier-mediated *p53* gene transfection could dramatically enhance the intracellular p53 expression level. Through *p53* gene delivery, obvious anti-proliferative effect could be detected which was elucidated to be associated with the simultaneous activation of mitochondrial-dependent apoptosis pathway and cell cycle arrest at G1 phase. Meanwhile, the anti-migration effect could be obtained after *p53* gene transfection.

Conclusion: Chol-*g*-PMSC-PPDL-mediated *p53* gene transfection could potentially be employed as a promising strategy for achieving effective anti-tumor response.

Keywords: cholesterol-*g*-poly(amine-co-ester), *p53* gene delivery, gene therapy, anti-proliferation effect, anti-migration effect

Introduction

Prostate cancer remains the most common diagnosed malignancy, which is a leading cause of cancer mortality in males worldwide.[1,2] Currently, the treatment of prostate cancer mainly depends on the nonspecific therapeutic strategies such as surgery and chemotherapy, in which high recurrence and drug resistance are difficult to be avoided.[3,4] In contrast, gene therapy has been considered to possess the potential in overcoming these limitations and thus widely accepted as an alternative approach in future cancer treatment.[5–7] In gene therapy, it is a crucial step to select an appropriate therapeutic gene. Among the therapeutic genes, tumor suppressor gene *p53* has been widely studied and identified to play a determinant role in diverse cell processes such as cell apoptosis, cell cycle regulation, and subsequent DNA repair.[8,9] Meanwhile, many studies have shown that the mutation and deficiency of *p53* gene exist in ~50% of human cancers, thereby leading to the apoptotic resistance and infinite proliferation of cancer cells.[10] Further, the restoration of wild-type *p53* gene could dramatically trigger the cell apoptosis and cell cycle arrest, particularly in the *p53*-deficient cells.[7] In addition, improving the expression level of *p53* gene in the *p53*-deficient cells could enhance the sensitivity to chemotherapeutics.[11] Thus, increasing the expression level

Correspondence: Dan Li
Department of Cancer Center, The First Hospital of Jilin University, Changchun 130021, People's Republic of China
Tel +86 431 8515 5201
Fax +86 431 8515 5200
Email lidan2009@jlu.edu.cn

Quanshun Li
Key Laboratory for Molecular Enzymology and Engineering of Ministry of Education, School of Life Sciences, Jilin University, Changchun 130012, People's Republic of China
Tel +86 431 8515 5201
Fax +86 431 8515 5200
Email quanshun@jlu.edu.cn

submit your manuscript | www.dovepress.com
Dovepress
http://dx.doi.org/10.2147/IJN.S191905

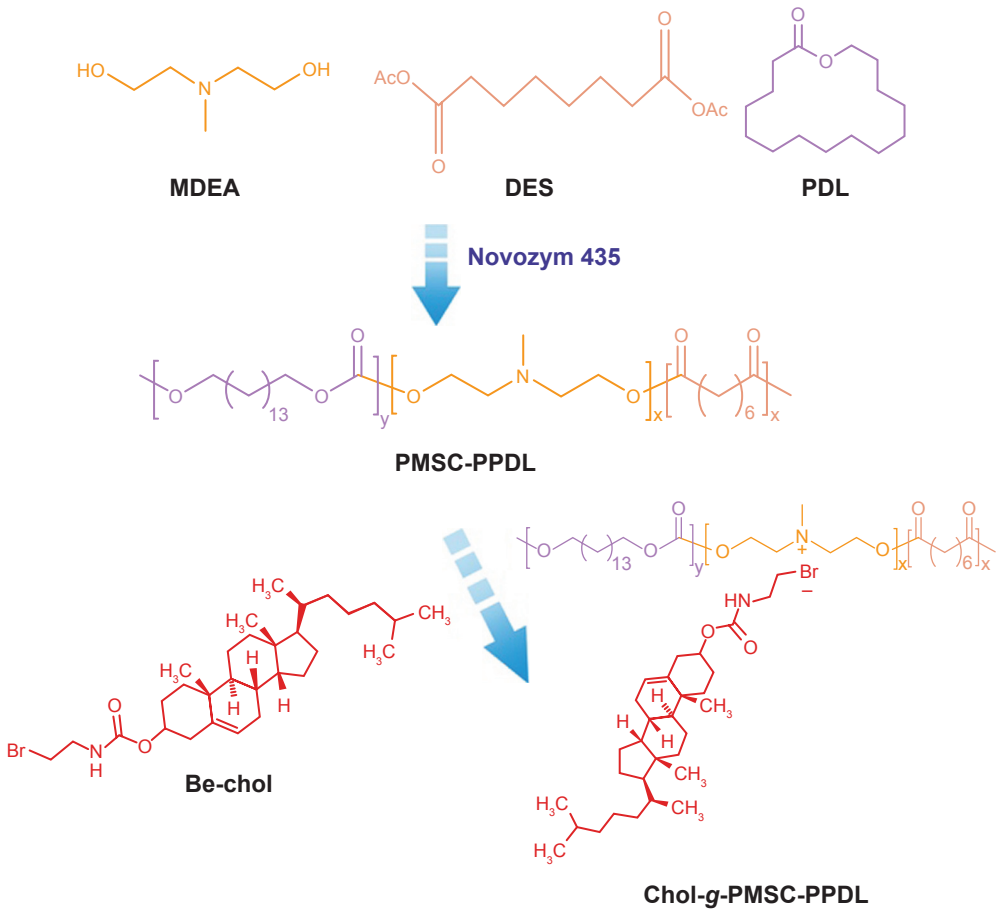

Scheme 1 Chemoenzymatic synthesis of Chol-*g*-PMSC-PPDL.

or activity of *p53* gene is expected to be an attractive means for achieving antitumor efficacy.

Besides the selection of therapeutic genes, the construction of gene carriers with high transfection efficiency and low cytotoxicity is another issue to be addressed in cancer gene therapy.[12,13] To date, cationic polymers such as poly(ethylenimine), polyamidoamine dendrimer, poly(L-lysine), and their derivatives have been successfully applied in *p53* gene delivery.[14–21] Apart from these cationic polymers, copolyester poly(amine-co-ester)s containing tertiary amino substituents have also been widely employed as gene vectors owing to their unique features such as high transfection efficiency, favorable biocompatibility and biodegradability, and ease of production.[22,23] Generally, poly(amine-co-ester)s are synthesized in a chemical manner, in which the trace residue and underlying toxicity of metallic catalysts may limit the clinical applications of products. Compared to chemical routes enzymatic polymerization has been considered to be a greener method for preparing polymeric materials due to its favorable characteristics of mild reaction conditions, no residue of metallic catalysts, high enantio-, chemo-, and regioselectivity, and convenient combination with chemical routes.[24–27] To date, several poly(amine-co-ester)s have been successfully synthesized by lipase-catalyzed ring-opening polymerization or polycondensation, and demonstrated to possess superior ability to transfer nucleic acids into mammalian cells.[22,23,28–30] In our previous study, a cationic amphiphilic copolymer cholesterol-*g*-poly(amine-co-ester), namely Chol-g-PMSC-PPDL has been successfully synthesized in a chemoenzymatic process and employed as a carrier in miR-23b delivery, which could achieve obvious anti-proliferation and anti-migration effects of tumor cells.[31,32]

Herein, the copolymer Chol-g-PMSC-PPDL obtained in a chemoenzymatic route (as shown in Scheme 1) was employed as a carrier for realizing *p53*-based gene therapy. The performance of *p53* gene transfection and the detailed mechanism of antitumor efficacy were subsequently evaluated using human prostate tumor cell line PC-3 (p53 null) as a model.

Materials and methods

Materials

The amphiphilic copolymer Chol-g-PMSC-PPDL was prepared from the *Candida antarctica* lipase (Novozym 435)-catalyzed

polymerization of N-methyldiethanolamine, diethyl sebacate, and ω-pentadecanolide and the subsequent chemical grafting reaction with cholesterol derivative according to our previous report.[31] The recombinant *Escherichia coli* DH5α harboring the plasmid p3XFLAG-CMV-p53 (encoding wild-type p53 protein) was stored in our laboratory, from which the plasmid was extracted using Axygen Plasmid Maxi kit (Corning Inc., Corning, NY, USA). Poly(ethylenimine) with a weight-average molecular weight of 25,000 g/mol (PEI25K) and crystal violet were obtained from Sigma-Aldrich Co. (St Louis, MO, USA). FBS and DMEM were purchased from Kangyuan Co. (Beijing, China) and Thermo Fisher Scientific (Waltham, MA, USA), respectively. MTT and TRNzol Universal reagent were purchased from AMRESCO, Inc. (Solon, OH, USA) and TIANGEN Biotech (Beijing) Co., Ltd. (Beijing, China), respectively. The primary antibodies (β-actin, procaspase-3, and p53 as targets) and horseradish peroxidase (HRP)-labeled secondary antibody were purchased from Abcam (Cambridge, UK). Other antibodies for detecting procaspase-8 and -9 were obtained from Cell Signaling Technology, Inc. (Danvers, MA, USA). Polyvinylidene fluoride (PVDF) membrane was purchased from EMD Millipore (Billerica, MA, USA). The kits used in the present study were obtained from the following companies: BCA protein assay kit, BioTeke (Beijing, China); JC-1 probe-based mitochondrial membrane potential kit, Beyotime Institute of Biotechnology (Jiangsu, China); caspase-3, -8, and -9 activity assay kits, Promega Corporation (Fitchburg, WI, USA); PrimeScript™ RT reagent kit and SYBR™ Premix Ex Taq kit, TaKaRa Bio Inc. (Kusatsu, Japan); live/dead viability/cytotoxicity kit, Thermo Fisher Scientific; and Annexin V-FITC/PI apoptosis and PI cell cycle detection kits, BestBio (Shanghai, China).

Gel retardation assay

The DNA binding and condensation ability of Chol-g-PMSC-PPDL was conducted by gel retardation assay. Briefly, Chol-g-PMSC-PPDL and p3XFLAG-CMV-p53 plasmid were gently mixed together at different mass ratios and incubated at room temperature for 30 minutes to obtain nanoparticles. The formed nanoparticles were then loaded to 1% agarose gel and electrophoresed in Tris-acetate-EDTA buffer (120 V, 10 minutes). To evaluate the stability of nanoparticles, Chol-g-PMSC-PPDL/p53 nanoparticle at a mass ratio of 40.0 was treated with DNase I solution (final concentration of 10 μg/mL) at 37°C for 15 minutes. Finally, 50 mg/mL of heparin solution was added into the mixture, and the samples were subjected to 1% agarose gel electrophoresis as described above. The gel was dyed with ethidium bromide and captured by the Universal Hood II imaging system (Bio-Rad Laboratories Inc., Hercules, CA, USA).

Intracellular distribution analysis of nanoparticles

The PC-3 cells were obtained from the Shanghai Institute of Cell Bank (Shanghai, China) and seeded into 6-well plates at a density of 2.0×10^5 cells/well. After this culture, with a sterilized coverslip for 24 hours, the cells were then cultured with 1 mL FBS-free medium containing Chol-g-PMSC-PPDL/TOTO-3-labeled p53 nanoparticles (mass ratio of 40.0) for 1, 2, 4, and 6 hours. The cells were then stained with LysoTracker Green for 30 minutes, washed with PBS thrice, fixed with cold 75% ethanol at 4°C for 20 minutes, and stained with DAPI solution. Finally, the coverslips were taken from the wells and observed using LSM 710 confocal laser scanning microscope (Carl Zeiss Meditec AG, Jena, Germany).

Real-time quantitative PCR (RT-qPCR)

PC-3 cells were cultured in DMEM supplemented with 10% FBS at 37°C in humidified air with 5% CO_2. The cells were seeded in 6-well plates at a density of 2.0×10^5 cells/well and transfected with different nanoparticles harboring 2.5 μg/mL of plasmid p3XFLAG-CMV-p53 in FBS-free DMEM for 6 hours (mass ratio of 40 and 1.33 for Chol-g-PMSC-PPDL and PEI25K, respectively). Afterward the cells were cultured in 10% FBS-containing DMEM for additional 48 hours, and total RNAs were isolated using TRNzol Universal reagent according to the manufacturer's instructions. The cDNA was synthesized from 1 μg of purified RNA as the template, using PrimeScript RT reagent kit with gDNA eraser. Using the obtained cDNA as template, the classical PCR amplification was conducted under the following conditions: 1 cycle at 94°C for 2 minutes and 30 cycles at 94°C for 30 seconds, 55°C for 30 seconds, and 72°C for 1 minute. Finally, RT-qPCR was carried out for 40 cycles (95°C for 5 seconds and 60°C for 34 seconds) using SYBR™ Premix Ex Taq kit on an 7500 RT-PCR Instrument (Thermo Fisher Scientific). The relative expression of *p53* gene was calculated and normalized by $2^{-\Delta\Delta CT}$ method, using *β-actin* as a reference gene. The primers were used as follows:

β-actin forward: 5′-TCTGGCACCACACCTTCTACAATG-3′;

reverse: 5′-GGATAGCACAGCCTGGATAGCAA-3′;

p53 forward: 5′-GGCTCTGACTGTACCACCATCCA-3′;

reverse: 5′-GGCACAAACACGCACCTCAAAG-3′.

Western blotting analysis

The cell culture and *p53* gene transfection were performed as described in section "Real-time quantitative PCR (RT-qPCR)." The cultured PC-3 cells were collected, washed with PBS thrice, and subjected to the lysis in RIPA buffer containing 1 mM phenylmethanesulfonyl fluoride on ice for 1 hour. The supernatants were collected through the centrifugation at 12,000 rpm for 10 minutes (4°C), and protein concentration was measured by BCA protein assay kit. Subsequently, 12% SDS-PAGE was conducted to separate the proteins, which were then transferred onto PVDF membrane. The membrane was incubated with PBST (0.1% Tween in PBS) containing 5% milk at room temperature for 2 hours and further treated with primary antibodies-containing PBS at 4°C overnight. Afterwards the membrane was washed with PBST thrice and incubated with HRP-labeled secondary antibody at room temperature for 1 hour. Finally, the expression level of specific proteins was detected by enhanced chemical luminescence (TransGen, Beijing, China) on a 2500 chemiluminescence imaging system (Tanon, Shanghai, China).

Cytotoxicity and anti-proliferation assay

The in vitro cytotoxicity of carrier and the inhibition of cell proliferation induced by p53 transfection were evaluated by MTT method. Briefly, PC-3 cells were seeded into 96-well plates at a density of 5,000 cells/well and cultured in 10% FBS-containing DMEM (200 μL) at 37°C for 24 hours. For in vitro cytotoxicity assay, the cells were treated with different concentrations of carriers (2–170 μg/mL) in 10% FBS-containing DMEM (200 μL) at 37°C for 48 hours. For the anti-proliferation assay, the cells were transfected with nanocomplexes containing 2.5 μg/mL of plasmid in FBS-free DMEM (200 μL) for 6 hours, and cultured for further 48 hours after the system was replaced by 10% FBS-containing DMEM. The cells were then incubated with 20 μL of MTT solution (5 mg/mL in PBS) at 37°C for 4 hours, and the formed formazan crystals were dissolved by 150 μL dimethyl sulfoxide at room temperature for 10 minutes. The optical density at 492 nm was measured using a GF-M3000 microplate reader (Caihong Co., Shandong, China), and the cell viability was determined to be the absorbance ratio of treated and untreated cells.

Live/dead staining

The cell culture and p53 transfection was conducted as described in section "Real-time quantitative PCR (RT-qPCR)." The collected cells were rinsed with 500 μL PBS twice and subjected to the staining at room temperature for 30 minutes with 200 μL of live/dead reagent composed of 2 mM calcein AM and 4 mM ethidium homodimer. The images were obtained through the observation under IX73P1F fluorescence microscopy (Olympus Corporation, Tokyo, Japan).

Cell colony formation assay

The cell culture and p53 transfection was conducted as described in section "Real-time quantitative PCR (RT-qPCR)." The cells were digested with 0.25% trypsin solution and reseeded into 6-well plates at a density of 1.0×10^4 cells/well. After one week of the culture, the cells were treated with 70% cold ethanol at 4°C for 20 minutes and stained with 0.2% crystal violet solution, followed by the observation to record the colony formation under an IX73P1F fluorescence microscopy (Olympus Corporation). Finally, 33% acetic acid solution was employed to treat the cells, and the optical density at 578 nm was measured using GF-M3000 microplate reader.

Cell apoptosis and cell cycle arrest assay

The cell culture and p53 transfection was conducted as described in section "Real-time quantitative PCR (RT-qPCR)." According to the manufacture's protocols, the collected cells were subjected to Annexin V-FITC and PI dual staining, and the cell apoptosis was detected by flow cytometry on fluorescence activated cell sorting (FACS) Caliber (BD Bioscience, San Jose, CA, USA). For the cell cycle assay, the cells were first fixed with 75% cold ethanol at –20°C for 1 hour, washed with PBS twice and treated with RNase I (20 μL) at 37°C for 30 minutes prior to the PI staining. Finally, the cells were stained with PI solution (300 μL) at 4°C for additional 30 minutes in the dark, and the cell cycle was measured on FACSCaliber (BD Bioscience). The cell apoptosis and cell cycle ratios were analyzed through CellQuest Pro software (BD Bioscience).

Caspase activities assay

The activities of caspase-3, -8, and -9 after p53 transfection were measured using the corresponding assay kits. The cells were cultured and transfected with different nanocomplexes as described in section "Real-time quantitative PCR (RT-qPCR)." The cells were treated with 100 μL of lysis buffer, and the lysates were incubated with the corresponding substrates in the dark at room temperature for 2.5 hours. Based on the manufacturer's protocols, the caspase-3, -8, and -9 activities were determined through monitoring each sample's luminescence on an Infinite F200 Pro plate reader (TECAN, Männedorf, Switzerland).

Mitochondrial membrane potential detection

The cell culture and *p53* gene transfection was carried out as described in section "Real-time quantitative PCR (RT-qPCR)," and the mitochondrial membrane potential changes were detected using JC-1 probe. Typically, the collected cells were dyed with JC-1 probe provided in the detection kit at 37°C for 30 minutes. The mitochondrial membrane potential was finally examined by IX73P1F fluorescence microscopy (Olympus Corporation) after the cells were rinsed with PBS twice.

Inhibition of cell migration assay

The inhibition of cell migration after p53 transfection was evaluated by wound healing and Transwell migration assays. For wound healing assay, 95% confluence of monolayer PC-3 cells in 6-well plates was scratched with a 200-μL pipette tip to produce the wounds on the surface of each well. Then the cells were transfected with different nanocomplexes harboring 2.5 μg/mL of plasmid in FBS-free DMEM for 6 hours and cultured in 10% FBS-containing DMEM for 48 hours. Images of the initial wound and the movement of cells into the scratched area were captured by IX73P1F fluorescence microscopy (Olympus Corporation), and the average distance of cell migration was calculated based on three representative zones. In Transwell migration assay, the upper chamber of the 24-well Transwell with 8-μm pore size was subjected to the cell seeding (2.0×10^4 cells/well), and 700 μL of 10% FBS-containing DMEM was added into the lower chamber. The non-migrating cells on the upper side of membrane were removed by clean swabs after 24 hours. The cells on the lower side were treated with 70% ethanol for fixation and stained with 0.2% crystal violet followed by washing with PBS thrice, and the cell migration was assayed on an IX73P1F fluorescence microscopy (Olympus Corporation). Finally, the invaded cells were subjected to the treatment with 33% acetic acid, and the optical density at 578 nm was measured by a GF-M3000 microplate reader.

Statistical analysis

The statistical analysis was conducted using GraphPad Prism 6.0. Data were analyzed by one-tailed and unpaired Student's *t*-test, and statistical significance was considered if *P*-value was lower than 0.05 ($*P<0.05$ and $**P<0.01$).

Results and discussion

According to our previous study, the cationic amphiphilic copolymer Chol-g-PMSC-PPDL was successfully synthesized in a chemoenzymatic process (Scheme 1), and the structure and molecular weight were systematically characterized with ^{1}H NMR and gel permeation chromatography.[31] Next, we investigated the DNA binding and condensation ability of Chol-g-PMSC-PPDL through gel retardation assay. As shown in Figure S1, Chol-g-PMSC-PPDL could efficiently condense the plasmid above the mass ratio of 40.0, thereby leading to stable nanoparticles through the electrostatic interaction. Further, the protection against nuclease's degradation was then conducted by incubating the nanoparticles with DNase I (Figure S2). Clearly, the free plasmid could be easily digested by DNase I, while an obvious plasmid band could be detected for Chol-g-PMSC-PPDL/p53 nanoparticles following the DNase I digestion and the subsequent treatment of heparin solution, indicating that the carrier Chol-g-PMSC-PPDL could efficiently protect *p53* gene from the DNase degradation. Moreover, the hydrodynamic size and zeta potential values of nanoparticles have been measured through Malvern Nano ZS90 Zetasizer in our previous report.[31] The Chol-g-PMSC-PPDL/p53 nanoparticles possessed hydrodynamic diameter and zeta potential of 89.1 nm and +12.1 mV at a mass ratio of 40.0, respectively. The morphology of nanoparticles was evaluated through TEM characterization. As shown in Figure S3, the nanoparticles exhibited the spherical structure with a particle size of ~88.9 nm, which was consistent with the hydrodynamic diameter measurement and favorable for the subsequent transfection. Besides, the investigation of intracellular distribution of nanoparticles has been considered to be beneficial for understanding the transfection mechanism.[33] Particularly, the evaluation of endosomal escape ability is an important step in the period of transfection.[34] As illustrated in Figure 1, red fluorescence generated from the TOTO-3-labeled p53 plasmid could be observed in the first 2 hours, indicating the Chol-g-PMSC-PPDL/p53 nanoparticle uptake by tumor cells. Subsequently, an increasing red fluorescence signal could be detected in the cells at 4 hours post-transfection, while an obvious endosomal entrapment of the nanoparticles could be obtained simultaneously. Notably, most nanoparticles could escape from the endosomes at 6 hours post-transfection, implying that Chol-g-PMSC-PPDL could possess desirable endosomal escape ability, thereby making it beneficial for further transfection.

Meanwhile, the transfection efficiency of Chol-g-PMSC-PPDL has been approved to be comparable to or even better than PEI25K using miR-23b, pGL-3, and pEGFP-N3 as models, and the optimal mass ratio for plasmid transfection was determined to be 40 (nitrogen/phosphorus [N/P] ratio of

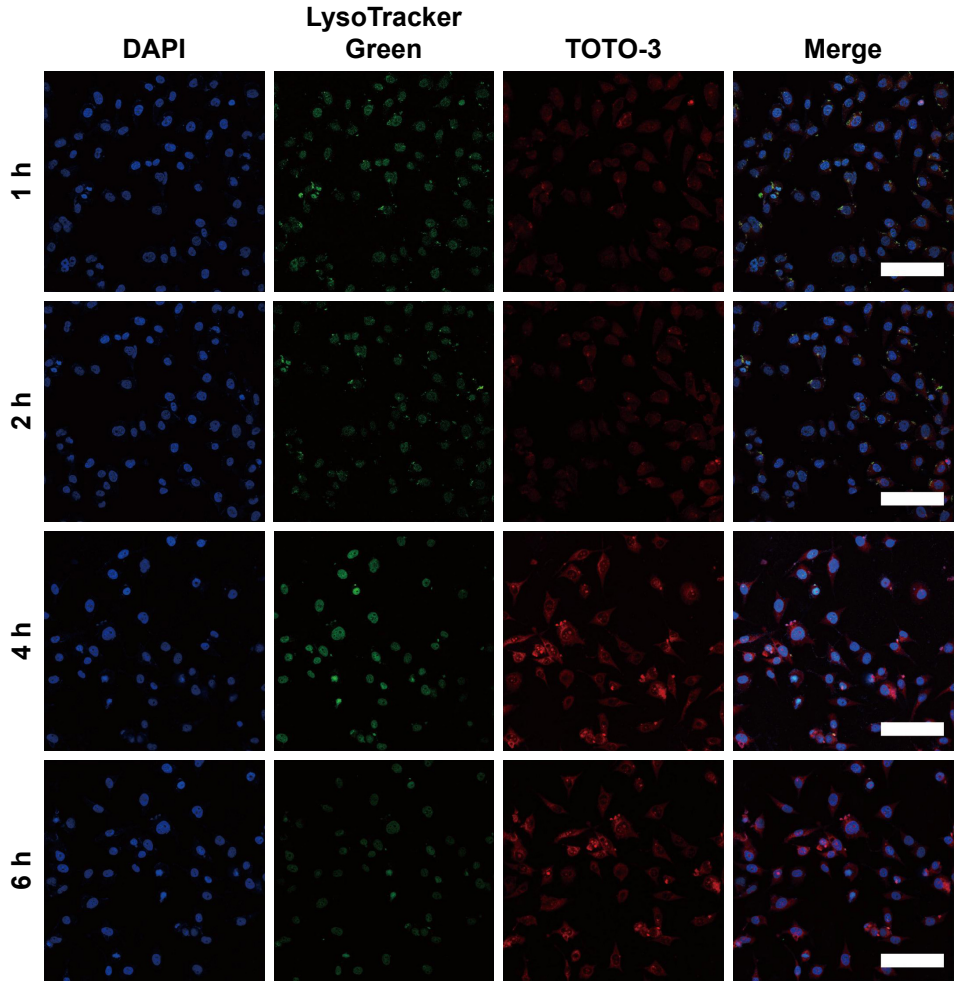

Figure 1 The intracelluar distribution of Chol-g-PMSC-PPDL/p53 nanoparticles at 1, 2, 4, and 6 hours.
Notes: Blue, DAPI; green, LysoTracker Green; red, TOTO-3-labeled p53 plasmid. The scale bar is 100 μm.

34.5).[31] In the present study, the copolymer Chol-g-PMSC-PPDL was employed as a carrier for *p53* gene transfection to achieve the antitumor efficacy in PC-3 cells. First, the in vitro cytotoxicity of Chol-g-PMSC-PPDL was measured in the concentration range of 2.0–170.0 μg/mL through MTT method. As shown in Figure S4, Chol-g-PMSC-PPDL exhibited much lower cytotoxicity than PEI25K at all the concentrations used, indicating its favorable biocompatibility. Higher cell viability could be obtained for Chol-g-PMSC-PPDL (>85%) at a concentration of 170 μg/mL, while <80% of cell viability was achieved for PEI25K at a concentration of 5 μg/mL. Then the *p53* gene transfection was evaluated at a mass ratio of 40 for Chol-g-PMSC-PPDL according to our previous report,[31] and mass ratio of 1.33 (equal to N/P ratio of 10) was employed for PEI25K, which has been widely accepted as its optimal ratio for transfection.[35] To check whether Chol-g-PMSC-PPDL could mediate efficient *p53* gene delivery, the transfection efficiency of *p53* gene in PC-3 cells was measured by RT-qPCR and Western blotting at mRNA and protein levels, respectively. As shown in Figure 2, no p53 expression could be detected in PC-3 cells owing to its intrinsic p53-null characteristic, and free plasmid transfection did not realize the improvement of p53 expression. However, the relative p53 mRNA level has been found to be increased by 115.0-fold after Chol-g-PMSC-PPDL-mediated p53 transfection, slightly higher than PEI25K/p53 group (106.1 fold). These results clearly showed that the carrier Chol-g-PMSC-PPDL could facilitate the *p53* gene delivery and further achieve the intracellular expression of *p53* gene. Further, the expression level of *p53* gene after transfection was measured by Western blotting (Figures 3 and S5). Negligible intracellular p53 protein expression has been observed in untreated PC-3 cells due to the p53-deficient state in this cell line. Compared to control and free plasmid groups, the p53 expression at protein level was significantly enhanced after PEI25K- and Chol-g-PMSC-PPDL-mediated

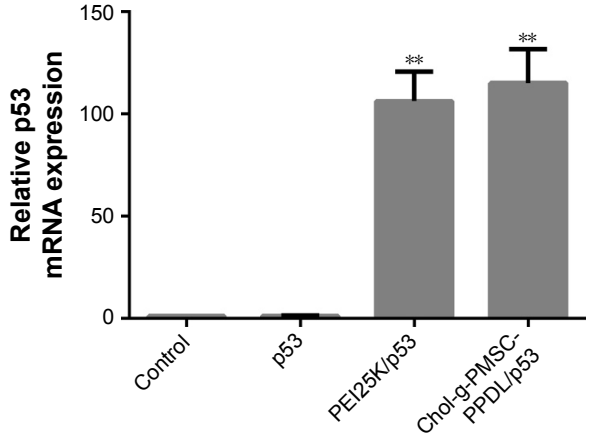

Figure 2 The p53 expression analysis at mRNA level after carrier-mediated p53 transfection through RT-qPCR analysis.
Note: Data are presented as mean value ± SD of triplicate experiments. $^{**}P<0.01$.
Abbreviation: RT-qPCR, real-time quantitative PCR.

p53 transfection. The results were consistent with RT-qPCR analysis, indicating that the exogenous *p53* gene delivery could enhance the expression of wild-type *p53* gene in tumor cells, and further achieve the *p53*-based gene therapy.

Since the *p53* gene transfection has been successfully achieved in PC-3 cells, the antiproliferative effect of Chol-g-PMSC-PPDL/p53 was then evaluated through MTT method (Figure 4). Compared to pEGFP-N3 plasmid transfection, the *p53* gene-based transfection could yield an obvious proliferative inhibition, indicating that the wild-type *p53* gene could exert the antiproliferative effect in prostate cancer cells. In PEI25K-mediated *p53* gene transfection, 32.83% of cell proliferation inhibition could be obtained, whereas Chol-g-PMSC-PPDL/p53 group exhibited much stronger inhibition of cell proliferation with an inhibition ratio of 45.49%. Meanwhile, superior anti-proliferation effect could

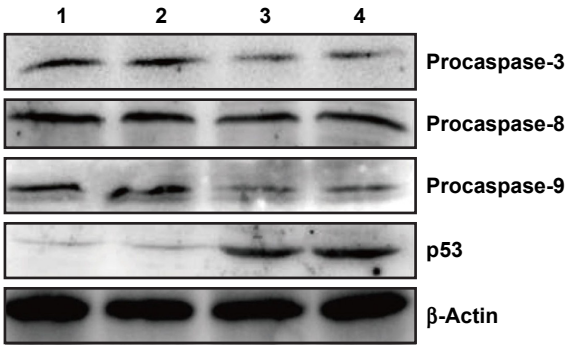

Figure 3 The expression levels of p53 and apoptosis-related proteins (procaspase-3, -8, and -9) by Western blotting.
Notes: Lane 1: control; lane 2: free p53 plasmid; lane 3: PEI25K/p53; and lane 4: Chol-g-PMSC-PPDL/p53.
Abbreviation: PEI25K, poly(ethylenimine) with a weight-average molecular weight of 25,000 g/mol.

be clearly observed at a mass ratio of 40, much higher than those at mass ratios of 30 and 50, which was in accordance with the optimal mass ratio of 40 in our previous report.[31] Thus, mass ratio of 40 was utilized in the following studies to elucidate the antitumor mechanism induced by p53 transfection. Further, live/dead staining assay was performed to get a direct evidence of the anti-proliferation effect, in which viable and dead cells were labeled to be green and red color owing to the intracellular enzymatic hydrolysis of calcein AM and the intercalation of ethidium homodimer to DNA, respectively.[36] As shown in Figure 5, almost no dead cells could be detected in the control and free plasmid groups since negligible red fluorescence could be obtained through fluorescence microscopic analysis. In contrast, obvious red fluorescence could be detected for Chol-g-PMSC-PPDL/p53 and PEI25K/p53 groups, and meanwhile stronger red signal could be found in Chol-g-PMSC-PPDL/p53 group implying that Chol-g-PMSC-PPDL-mediated *p53* gene transfection could induce significant apoptosis of PC-3 cells. Additionally, the colony formation assay was conducted to test the anti-proliferation effect of *p53* gene transfection (Figure S6). The Chol-g-PMSC-PPDL/p53 group could induce less formation of cell colonies, indicating that the antiproliferative effect could be achieved after Chol-g-PMSC-PPDL/p53 transfection. All these results demonstrated that Chol-g-PMSC-PPDL could efficiently deliver *p53* gene into PC-3 cells and further trigger the proliferation inhibition function of p53 protein. Meanwhile, Chol-g-PMSC-PPDL-mediated p53 delivery has been proved to possess stronger antiproliferative effect than PEI25K/p53 transfection.

In order to gain the deeper insight of the mechanism of anti-proliferation effect in PC-3 cells, the cell apoptosis was assayed by flow cytometry after the transfected cells were stained with Annexin V-FITC/PI solution. As shown in Figure 6, similar apoptotic ratio was obtained in the free plasmid group (1.71%) to control group (1.29%) suggesting that free plasmid did not induce the cell apoptosis. Remarkably, both PEI25K/p53 and Chol-g-PMSC-PPDL/p53 groups could trigger efficient early-stage apoptosis, with the apoptotic ratio of 53.98% and 54.90% in PC-3 cells, respectively. Apparently, the results showed that these two carrier-mediated p53 deliveries shared similar cell apoptotic ratios, which was not in agreement with the proliferation inhibition acquired in MTT assay. This phenomenon could be attributed to the fact that the intrinsic cytotoxicity of PEI25K could stimuli an enhanced apoptosis except for the p53-dependent apoptosis in cancer cells. In addition, the anti-proliferation effect was caused not just by the induction of

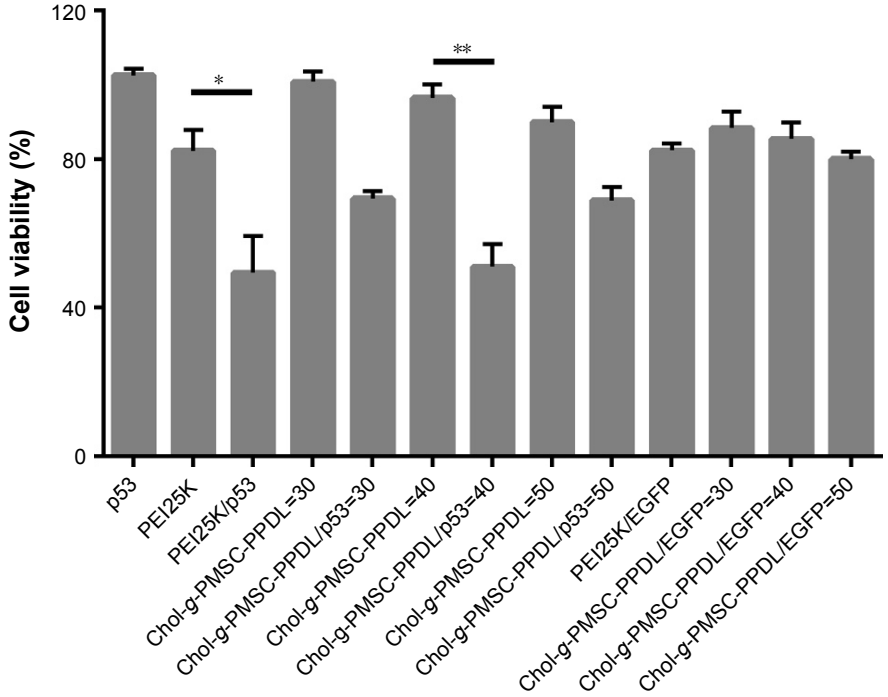

Figure 4 The cell viability assay after PEI25K- and Chol-*g*-PMSC-PPDL-mediated p53 transfection for 48 hours. The mass ratio of PEI25K/plasmid was 1.33. Data are presented as mean value ± SD of triplicate experiments. *$P<0.05$; **$P<0.01$.
Abbreviation: PEI25K, poly(ethylenimine) with a weight-average molecular weight of 25,000 g/mol.

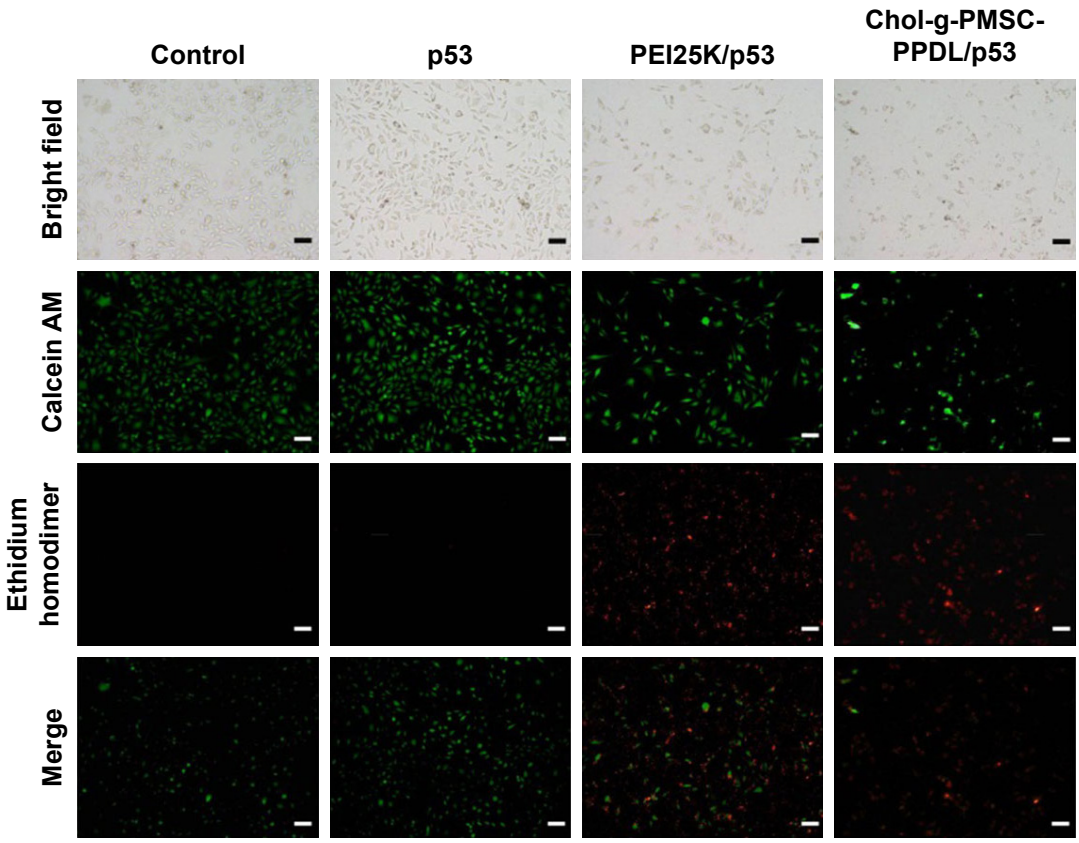

Figure 5 Live/dead staining of PC-3 cells after *p53* gene transfection.
Note: The scale bar is 100 μm.

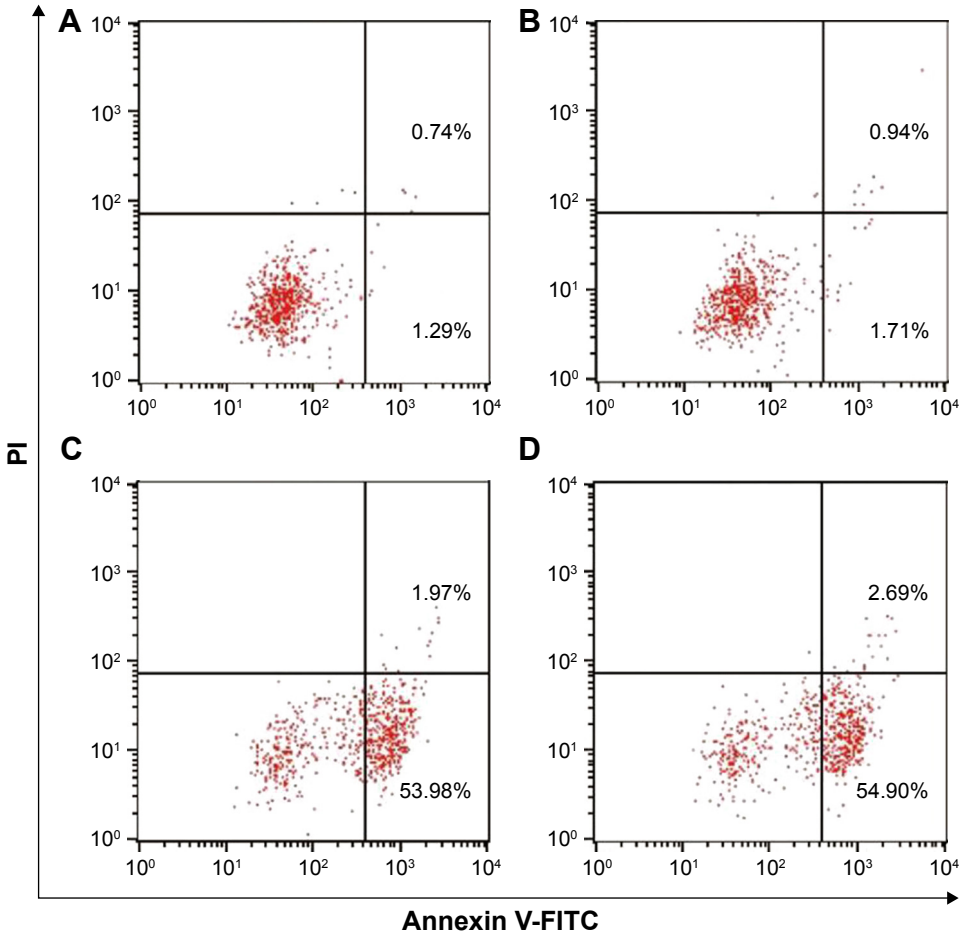

Figure 6 Flow cytometric analysis for the cell apoptosis after p53 transfection through Annexin V-FITC/PI staining: (**A**) control; (**B**) free p53 plasmid; (**C**) PEI25K/p53; and (**D**) Chol-*g*-PMSC-PPDL/p53.
Abbreviation: PEI25K, poly(ethylenimine) with a weight-average molecular weight of 25,000 g/mol.

cell apoptosis, but other mechanisms might also be involved in the induction of anti-proliferation effect such as cell cycle arrest. Thus, cell cycle arrest was subsequently determined using flow cytometry after *p53* gene delivery. As shown in Figure 7, after the transfection of exogenous *p53* gene using Chol-g-PMSC-PPDL or PEI25K, the G1 phase proportion of PC-3 cells appeared to have increased in comparison to the control group, demonstrating the presence of cell cycle arrest triggered by p53 expression. These results were in agreement with the general report that *p53* gene could induce antiproliferative effect by blocking the cell cycle at G1 or S phase.[37,38] It is worth to be noted that Chol-g-PMSC-PPDL/p53 group exhibited slightly higher ratio of G1 phase (57.06%) than PEI25K/p53 group (G1 ratio of 51.46%), implying a higher induction ability of cell cycle arrest. Thus, the relatively higher cell cycle arrest could contribute to the enhanced antiproliferative effect induced by Chol-g-PMSC-PPDL/p53 transfection, filling the gap between the difference in MTT assay and cell apoptosis analysis.

To further clarify the mechanism of apoptotic process, the expression level of apoptosis-related proteins (procaspase-3, -8, and -9) was determined by Western blotting. As shown in Figure 3, free plasmid transfection could not alter the expression level of procaspase-3, while both PEI25K/p53 and Chol-g-PMSC-PPDL/p53 groups could dramatically decrease the procaspase-3 expression. The cleavage of procaspase-3 meant the activation of caspase-3, which was considered to be a key role in caspase family-related apoptotic cascade to initiate the apoptotic process. Meanwhile, the procaspase-9 expression was obviously decreased after p53 transfection, suggesting that *p53*-mediated gene delivery could activate the caspase-9 expression and further trigger the mitochondrial-dependent apoptosis pathway. The enzymatic activities of caspase-3 and caspase-9 were detected using the corresponding kits indicating that both of them obviously increased after *p53* gene transfection (Figure S7), which was consistent with Western blotting. In addition, the mitochondrial membrane potential was measured after *p53* gene transfection using

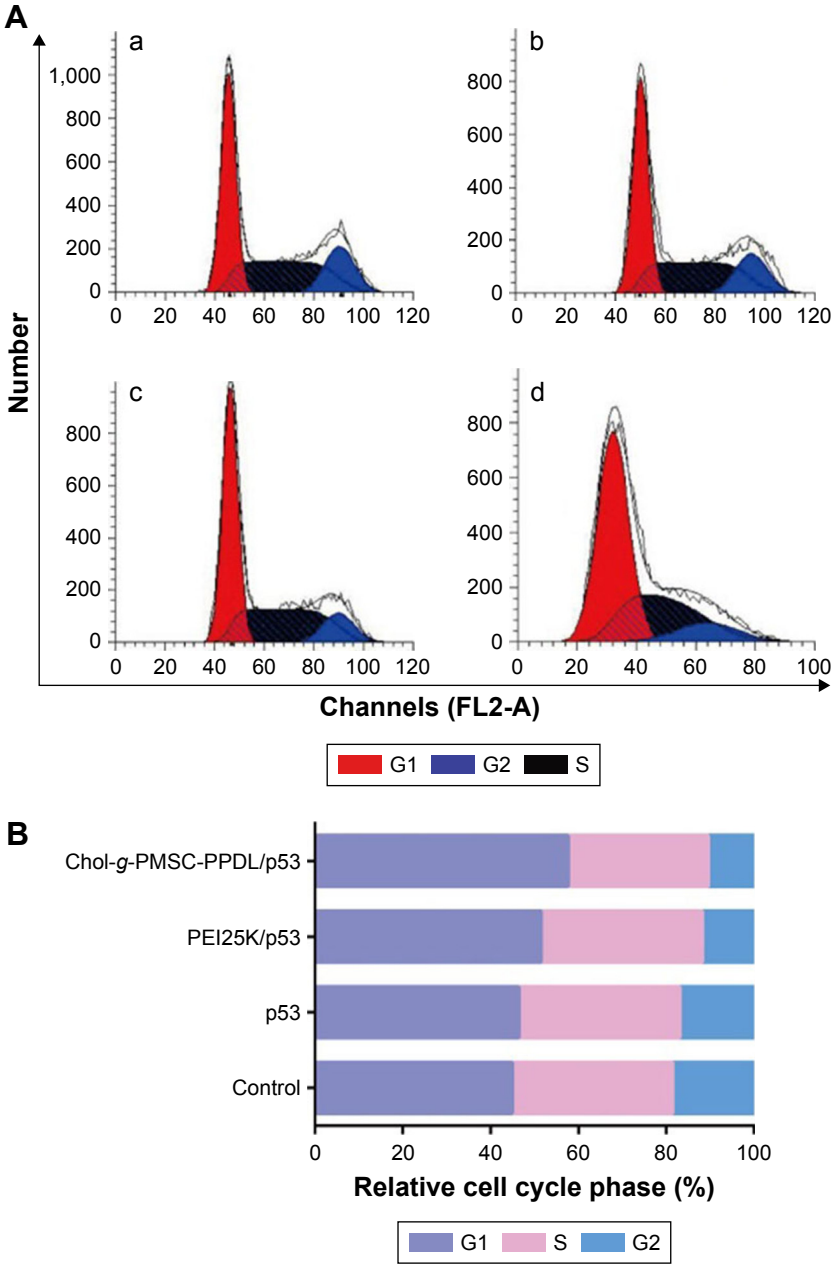

Figure 7 Flow cytometric analysis for the cell cycle arrest of PC-3 cells after p53 transfection through PI staining (**A**) and the quantitative analysis (**B**): (a) control; (b) free p53 plasmid; (c) PEI25K/p53; and (d) Chol-*g*-PMSC-PPDL/p53.
Abbreviation: PEI25K, poly(ethylenimine) with a weight-average molecular weight of 25,000 g/mol.

JC-1 probe (Figure S8). The green fluorescence that originated from monomeric JC-1 could be clearly observed in PEI25K/p53 and Chol-g-PMSC-PPDL/p53 groups, indicating the decreased mitochondrial membrane potential during the process of cell apoptosis. All these results demonstrated that the carrier-mediated p53 transfection could realize the apoptotic response in a mitochondrial-dependent signaling pathway. Although the expression level of procaspase-8 did not appear to be different in Western blotting assay, the activities of caspase-8 were measured to have enhanced after p53 delivery. The results were probably attributed to the detection of procaspase-8, not caspase-8 in Western blotting, which could not represent the accurate expression level of cleaved caspase-8. The enhanced activity of caspase-8 could demonstrate that the carrier-mediated p53 transfection in PC-3 cells could also launch the death receptor-mediated apoptosis pathway.

Finally, the inhibition of cell migration after p53 transfection was evaluated through wound healing and Transwell migration assay. As shown in Figure 8, the cells constantly

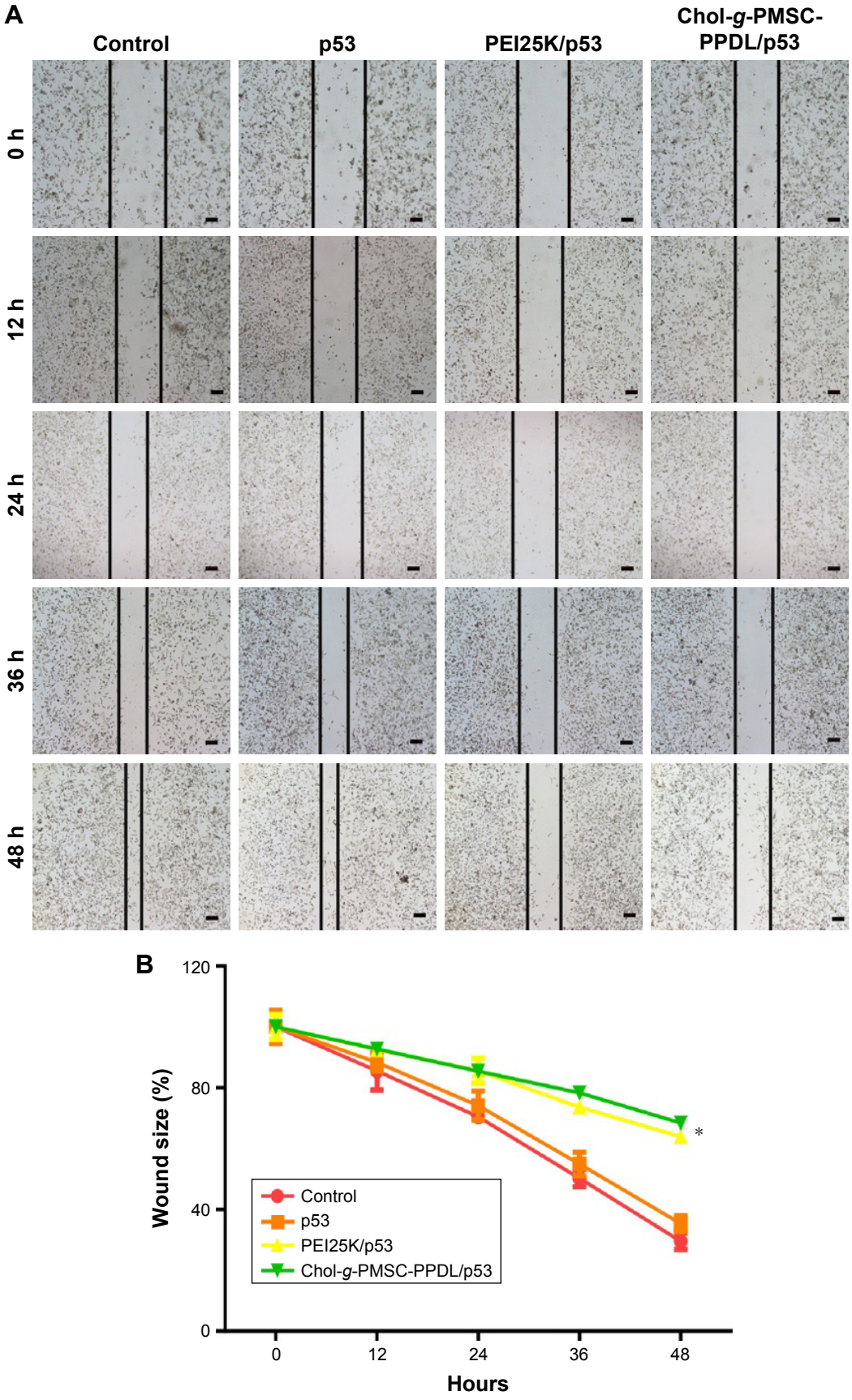

Figure 8 Wound healing assay of PC-3 cells after p53 transfection for different time (**A**) and the quantitative analysis of wound size (**B**).
Notes: Data are presented as mean value ± SD of triplicate experiments. *$P<0.05$. The scale bar is 100 μm.
Abbreviation: PEI25K, poly(ethylenimine) with a weight-average molecular weight of 25,000 g/mol.

migrated to the scratched area in control and free plasmid groups during 48 hours, and high density of cells could induce the cell death to some extent. As shown in Figure 7, the cells constantly migrated to the scratched area in control and free plasmid groups during 48 hours. Nevertheless, wider wound size was still presented in both Chol-g-PMSC-PPDL/p53 and PEI25K/p53 groups, indicating that the successful p53 expression could achieve higher anti-migration effect of tumor cells. Similarly, PC-3 cells exhibited much lower invasive ability to cross the membrane to the lower side after *p53* gene transfection in Transwell migration assay, in which Chol-g-PMSC-PPDL-mediated p53 transfection showed higher inhibition on migration and invasion than PEI25K (Figure S9). Thus, we concluded that the p53 transfection mediated by Chol-g-PMSC-PPDL could meanwhile inhibit the proliferation and migration, which provided an effective strategy for achieving the gene therapy of metastasis-related malignant tumors.

Conclusion

In summary, an amphiphilic copolymer cholesterol-*g*-poly(amine-co-ester) obtained in a chemoenzymatic route was successfully applied in the *p53* gene delivery for realizing the gene therapy of prostate tumor cells. Compared to PEI25K, Chol-g-PMSC-PPDL exhibited relatively higher p53 transfection efficiency and lower cytotoxicity. Through the successful intracellular p53 expression, obvious anti-proliferation and anti-migration effects could be achieved to attain the goal of tumor treatment in which the anti-proliferation was identified to be associated with the induction of cell apoptosis and cell cycle arrest at G1 phase. Thus, the cationic poly(amine-co-ester) derivative could potentially be used as an effective gene carrier for treating cancers and other malignant diseases. The in vivo evaluation and detailed mechanism analysis of carrier-mediated p53 delivery is still underway in our laboratory.

Acknowledgment

The authors gratefully acknowledge the support from the National Key R&D Program of China (2018YFC1105401), National Natural Science Foundation of China (81673502 and 81872928), Province-University Cooperation Project of Jilin Province (SXGJQY2017-4), Science & Technology Department of Jilin Province (20190201288JC), Education Department of Jilin Province (JJKH20190010KJ), and Graduate Innovation Program of Jilin University (101832018C182).

Disclosure

The authors report no conflicts of interest in this work.

References

1. Gundem G, Van Loo P, Kremeyer B, et al. The evolutionary history of lethal metastatic prostate cancer. *Nature*. 2015;520(7547):353–357.
2. Bruinsma SM, Bangma CH, Carroll PR, et al. Active surveillance for prostate cancer: a narrative review of clinical guidelines. *Nat Rev Urol*. 2016;13(3):151–167.
3. Hamdy FC, Donovan JL, Lane JA, et al. 10-Year outcomes after monitoring, surgery, or radiotherapy for localized prostate cancer. *N Engl J Med*. 2016;375(15):1415–1424.
4. Holohan C, Van Schaeybroeck S, Longley DB, Johnston PG. Cancer drug resistance: an evolving paradigm. *Nat Rev Cancer*. 2013;13(10):714–726.
5. Niidome T, Huang L. Gene therapy progress and prospects: nonviral vectors. *Gene Ther*. 2002;9(24):1647–1652.
6. Yin H, Kanasty RL, Eltoukhy AA, et al. Non-viral vectors for gene-based therapy. *Nat Rev Genet*. 2014;15(8):541–555.
7. Han H, Chen W, Yang J, et al. Inhibition of cell proliferation and migration through nucleobase-modified polyamidoamine-mediated p53 delivery. *Int J Nanomed*. 2018;13:1297–1311.
8. Li Y, Xu B, Bai T, Liu W. Co-delivery of doxorubicin and tumor-suppressing p53 gene using a POSS-based star-shaped polymer for cancer therapy. *Biomaterials*. 2015;55:12–23.
9. Muller PA, Vousden KH. Mutant p53 in cancer: new functions and therapeutic opportunities. *Cancer Cell*. 2014;25(3):304–317.
10. Rivlin N, Brosh R, Oren M, Rotter V, et al. Mutations in the p53 tumor suppressor gene: important milestones at the various steps of tumorigenesis. *Genes Cancer*. 2011;2(4):466–474.
11. Liu C, Zhu Y, Lou W, et al. Functional p53 determines docetaxel sensitivity in prostate cancer cells. *The Prostate*. 2013;73(4):418–427.
12. Li SD, Huang L. Gene therapy progress and prospects: non-viral gene therapy by systemic delivery. *Gene Ther*. 2006;13(18):1313–1319.
13. Zhang J, Wang Y, Chen J, et al. Inhibition of cell proliferation through an ATP-responsive co-delivery system of doxorubicin and Bcl-2 siRNA. *Int J Nanomed*. 2017;12:4721–4732.
14. Zhang J, Wu D, Xing Z, et al. N-Isopropylacrylamide-modified polyethylenimine-mediated p53 gene delivery to prevent the proliferation of cancer cells. *Colloids and Surfaces B: Biointerfaces*. 2015;129:54–62.
15. Li Z, Zhang L, Li Q. Induction of apoptosis in cancer cells through N-acetyl-l-leucine-modified polyethylenimine-mediated p53 gene delivery. *Colloids and Surf B Biointerfaces*. 2015;135:630–638.
16. Han H, Yang J, Wang Y, et al. Nucleobase-modified polyamidoamine-mediated miR-23b delivery to inhibit the proliferation and migration of lung cancer. *Biomater Sci*. 2017;5(11):2268–2275.
17. Xing Z, Gao S, Duan Y, et al. Delivery of DNAzyme targeting Aurora kinase A to inhibit the proliferation and migration of human prostate cancer. *Int J Nanomed*. 2015;10:5715–5727.
18. Guan X, Li Y, Jiao Z, et al. Codelivery of antitumor drug and gene by a pH-sensitive charge-conversion system. *ACS Appl Mater Interfaces*. 2015;7(5):3207–3215.
19. Li J, Liang H, Liu J, Wang Z. Poly (amidoamine) (PAMAM) dendrimer mediated delivery of drug and pDNA/siRNA for cancer therapy. *Int J Pharm*. 2018;546(1–2):215–225.
20. Cheng WJ, Chen LC, Ho HO, Lin HL, Sheu MT. Stearyl polyethylenimine complexed with plasmids as the core of human serum albumin nanoparticles noncovalently bound to CRISPR/Cas9 plasmids or siRNA for disrupting or silencing PD-L1 expression for immunotherapy. *Int J Nanomed*. 2018;13:7079–7094.
21. Johnson RP, Uthaman S, John JV, et al. Poly(2-hydroxyethyl methacrylate)-*b*-poly(L-Lysine) cationic hybrid materials for non-viral gene delivery in NIH 3T3 mouse embryonic fibroblasts. *Macromol Biosci*. 2014;14(9):1239–1248.

22. Zhou J, Liu J, Cheng CJ, et al. Biodegradable poly(amine-co-ester) terpolymers for targeted gene delivery. *Nat Mater*. 2012;11(1):82–90.
23. Jiang Y, Gaudin A, Zhang J, et al. A "top-down" approach to actuate poly(amine-co-ester) terpolymers for potent and safe mRNA delivery. *Biomaterials*. 2018;176:122–130.
24. Kobayashi S. Recent developments in lipase-catalyzed synthesis of polyesters. *Macromol Rapid Commun*. 2009;30(4–5):237–266.
25. Kobayashi S, Makino A. Enzymatic polymer synthesis: an opportunity for green polymer chemistry. *Chem Rev*. 2009;109(11):5288–5353.
26. Yang Y, Zhang J, Wu D, et al. Chemoenzymatic synthesis of polymeric materials using lipases as catalysts: a review. *Biotechnol Adv*. 2014; 32(3):642–651.
27. Shoda S, Uyama H, Kadokawa J, Kimura S, Kobayashi S. Enzymes as green catalysts for precision macromolecular synthesis. *Chem Rev*. 2016;116(4):2307–2413.
28. Zhang J, Cui J, Deng Y, Jiang Z, Saltzman WM. Multifunctional Poly(amine-co-ester-*co*-ortho ester) for Efficient and Safe Gene Delivery. *ACS Biomater Sci Eng*. 2016;2(11):2080–2089.
29. Yang Z, Jiang Z, Cao Z, et al. Multifunctional non-viral gene vectors with enhanced stability, improved cellular and nuclear uptake capability, and increased transfection efficiency. *Nanoscale*. 2014;6(17):10193–10206.
30. Cui J, Qin L, Zhang J, et al. *Ex vivo* pretreatment of human vessels with siRNA nanoparticles provides protein silencing in endothelial cells. *Nat Commun*. 2017;8(1):191.
31. Chen J, Jiang W, Han H, et al. Chemoenzymatic Synthesis of Cholesterol-*g*-Poly(amine-*co*-ester) Amphiphilic Copolymer as a Carrier for miR-23b Delivery. *ACS Macro Lett*. 2017;6(5):523–528.
32. Dong M, Chen J, Yang J, et al. Chemoenzymatic synthesis of a cholesterol-*g*-poly(amine-*co*-ester) carrier for p53 gene delivery to inhibit the proliferation and migration of tumor cells. *New J Chem*. 2018; 42(16):13541–13548.
33. Liu J, Li J, Liu N, et al. *In vitro* studies of phospholipid-modified PAMAM-siMDR1 complexes for the reversal of multidrug resistance in human breast cancer cells. *Int J Pharm*. 2017;530(1–2):291–299.
34. Li J, Liu J, Guo N, Zhang X. Reversal of multidrug resistance in breast cancer MCF-7/ADR cells by h-R3-siMDR1-PAMAM complexes. *Int J Pharm*. 2016;511(1):436–445.
35. Tian H, Li F, Chen J, Huang Y, Chen X. *N*-isopropylacrylamide-modified polyethylenimines as effective gene carriers. *Macromol Biosci*. 2012;12(12):1680–1688.
36. Wu D, Wang C, Yang J, et al. Improving the intracellular drug concentration in lung cancer treatment through the Codelivery of doxorubicin and miR-519c mediated by porous PLGA microparticle. *Mol Pharm*. 2016;13(11):3925–3933.
37. Pietenpol JA, Stewart ZA. Cell cycle checkpoint signaling: cell cycle arrest versus apoptosis. *Toxicology*. 2002;181–182:475–481.
38. Engeland K. Cell cycle arrest through indirect transcriptional repression by p53: I have a dream. *Cell Death Differ*. 2018;25(1):114–132.